On the Upper and Lower Bounds of Correlation Window Size in Digital Image Correlation Analysis

Hongjia Zhang, Melanie Senn, Tan Sui, Alexander Lunt, León Romano Brandt, Chrysanthi Papadaki, Siqi Ying, Enrico Salvati, Chris Eberl and Alexander M. Korsunsky*

***Abstract*—Digital Image Correlation (DIC), as a technique based on image processing, has been intensively used for displacement measurement. The setup of DIC analysis starting condition is crucial to the validity of the results. In this paper, the influence of correlation window size (*corrsize*), one of the parameters that need to be chosen by users for setup, is studied. The results show that DIC is reliable as long as the *corrsize* is between a lower bound ($corssize_{min}$) and an upper bound ($corssize_{max}$). The reason why DIC returns high error factor when beyond $corssize_{max}$ is related to image boundary effect, which is demonstrated by an equation serving as a criterion for *corrsize* choice. The study in this paper is particularly vital in cases where the Region of Interest (ROI) is close to the image and the real displacement is large.**

***Index Terms*—Digital Image Correlation, Correlation Window Size, Upper and Lower Bounds, Image Boundary Effect**

I. Introduction

Digital Image Correlation (DIC) has drawn a great deal of attention in the field of experimental mechanics due to its capability to measure in-plane full-field displacements with sub-pixel accuracy [1]. DIC finds a wide range of applications in displacement measurement both at the macroscopic [2, 3] and microscopic [4-10] levels. Particularly, in recent years, the combination of Focused Ion Beam (FIB) and DIC has become established as a new method for the evaluation of residual stress at the micro-scale [11-16]. Compared to conventional strain measurement methods such as strain gauge techniques, DIC image capture has the advantage of being economical and can be performed within the microscope, outdoors in the civil engineering context, etc., making *in situ* experiments a lot easier [2]. A principal benefit of DIC its non-contact nature that is particularly advantageous when measurement has to be performed over large distances or samples are too fragile to be attached to displacement sensors.

There is a variety of DIC implementations available commercially and within the academic context. The present paper specifically focused on the DIC package developed by C. Eberl and M. Senn [17], and adapted further within the framework of EU project iStress. This package is based on Matlab implementation. The advantage of this package lies in the combination of having a compiled version together with the original code. On the one hand, the compiled version allows an easier experience with a friendly interface (Fig. 1). Moreover, the graphical interface saves the users a considerable amount of time by sparing the effort of putting commands in the Matlab window. On the other hand, with the original code provided, users can modify them to achieve special purposes.

To ensure accurate results, the starting conditions of DIC analysis, including image filter and marker position, should be selected with caution. In this paper the influence of one of these parameters '*corrsize*' has been investigated. 'Corrsize' is short for 'correlation window size', and is defined as half of the length of one of the sides of the square correlation window which is used for image comparison. Instead of using the whole image, this sub-image is used to enhance the efficiency of DIC. In theory, as long as *corrsize* is large enough for the correlation region to cover the real displacement, DIC should give reliable results. In reality, image boundary effect also has to be taken into consideration and therefore further investigation has been performed, as outlined below.

Manuscript received March 21, 2017; revised April 19, 2017. This work was partially supported by EPSRC via grants EP/I020691, as well as by EU FP7 project iSTRESS (604646), EP/H003215 and EP/G004676.

Hongjia Zhang is a PhD student at Department of Engineering Science, University of Oxford, OX1 3PJ, UK. (e-mail: hongjia.zhang@eng.ox.ac.uk).

Melanie Senn was a postdoctoral research assistant at Fraunhofer Institute for Mechanics of Materials IWM, 79108, Germany. (e-mail: melanie.senn@gmail.com).

Tan Sui is a senior researcher in engineering and microscopy at Department of Engineering Science, University of Oxford, OX1 3PJ, UK. (e-mail: tan.sui@eng.ox.ac.uk).

Alexander Lunt is a senior fellow at European Organization for Nuclear Research (CERN), CH-1211, Switzerland. (e-mail: alexander.lunt@cern.ch).

León Romano Brandt is a PhD student at Department of Engineering Science, University of Oxford, OX1 3PJ, UK. (e-mail: leon.romanobrandt@eng.ox.ac.uk).

Chrysanthi Papadaki is a PhD student at Department of Engineering Science, University of Oxford, OX1 3PJ, UK. (e-mail: Chrysanthi.papadaki @eng.ox.ac.uk).

Siqi Ying is a PhD student at Department of Engineering Science, University of Oxford, OX1 3PJ, UK. (e-mail: siqi.ying@eng.ox.ac.uk).

Enrico Salvati is a PhD student at Department of Engineering Science, University of Oxford, OX1 3PJ, UK. (e-mail: enrico.salvati@eng.ox.ac.uk).

Chris Eberl is a professor at Fraunhofer Institute for Mechanics of Materials IWM, 79108, Germany.(e-mail: chris.eberl@iwm.fraunhofer.de).

*Alexander M. Korsunsky is a professor at Department of Engineering Science, University of Oxford, OX1 3PJ, UK. (tel: +44 1865273043; e-mail: alexander.korsunsky@eng.ox.ac.uk)

ISBN: 978-988-14047-4-9
ISSN: 2078-0958 (Print); ISSN: 2078-0966 (Online)

II. Experiment

A. DIC Analysis Description

Fig. 1 is the interface of DIC in use. Three main procedures are included in a DIC analysis: preprocessing, processing and postprocessing. At preprocessing, the processing conditions are selected in order to optimize the analysis performed. This includes preparing image sequence, selecting the image filter, placing markers and checking the quality of the images. The *corrsize* parameter is also selected before marker tracking is implemented. Postprocessing is then performed to clean the markers according to the correlation coefficient or standard deviation of fitting. Calculations can then be performed to determine the strain-field or displacement-field of the region of interest.

DIC analysis is typically performed on an array of images,

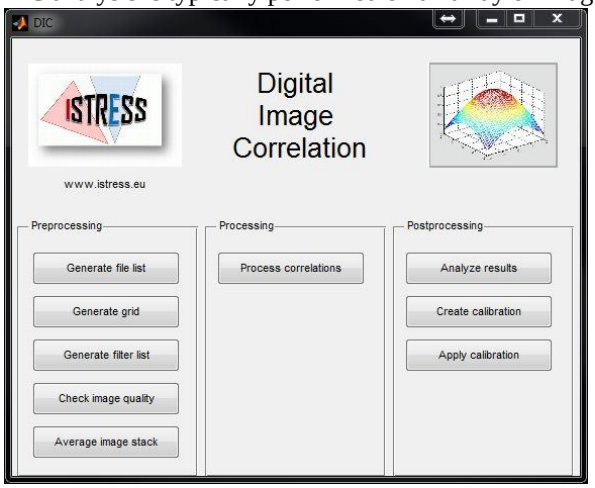

Fig. 1. Graphical interface of the compiled DIC

the first image being the base image and the rest being deformed or displaced versions of this original[18]. 'Deformed' here merely refers to the content of the image (i.e., the sample surface in the case of FIB-DIC ringcore milling[6]) rather than the image itself. Region of Interest (ROI) on the image is defined through placing tracking markers on the base image accordingly. By comparing the sequence of deformed images with the base image, displacement field of ROI in each deformed image is obtained in the form of x- and y- displacement of each marker. In order to compare the deformed images with the base image, the ROI surrounding each marker is compared with the base image by calculating the cross-correlation surface over a pre-defined window. Essentially this can be considered as if the deformed image is looking for the best match to the original image in a pixel-by-pixel search[18]. In the Matlab implementation of this code the cross-correlation surface is obtained using the 2D normalized cross-correlation in 'nomxcorr2.m'[19, 20]. The new position of the ROI is decided by fitting the cross-correlation surface to find the best possible match, as described in more detail elsewhere[18].

The pre-defined window mentioned above is the correlation window introduced earlier in this paper. Correlation window is centred on an individual marker and its size is associated with the parameter '*corrsize*' (Fig. 3).

B. Study of Correlation Window Size Influence

In order to simplify the investigation into *corrsize*, DIC was performed using the base image and only one deformed image, as illustrated in Fig. 2(a). During the analysis the ROI was centered on the one and only single white pixel which was located at position (x_0, y_0). Note that the position is counted in pixel. Moreover, x_0, y_0 respectively represent the distance from the pixel to the left boundary and to the top boundary of the image. The deformed image is only a shift of the base image by d (pixels) and d (pixels) along x- and y-direction respectively. In Fig. 2(a) d is 10pixels and (x_0, y_0) is (55, 56) as an example, resulting in the new position of (65, 66) of the white pixel in the deformed image. Therefore, the intensity levels in the base image and the deformed image are identical. d will be defined as the real displacement in the following discussion. Fig. 2(b) is the 3D surface plot of the area in red dashed rectangle in Fig. 2(a). It shows that the white pixel is a unique and outstanding feature in the whole image. This is to ensure that no confusion is caused between pixels with similar intensity level during cross-correlation. Fig. 3 depicts the marker position and the correlation window on the base image when *corrsize* is 12pixels as an example. Only one marker was placed in the middle of the white pixel for simplicity. The top right inset is the figure of marker position with higher resolution. The size of the correlation window (the orange rectangle) equals to 2**corrsize*+1, including one pixel that the marker occupies. Hence the side length of the correlation window in Fig. 3 is 25pixels.

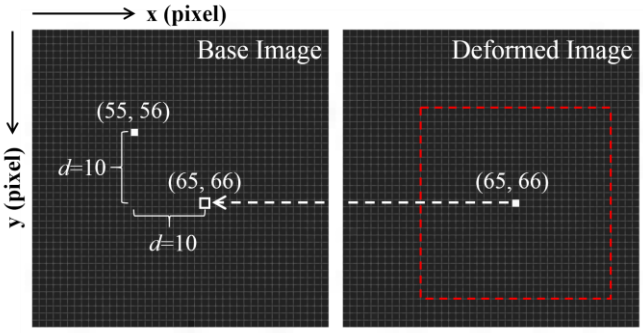

(a)

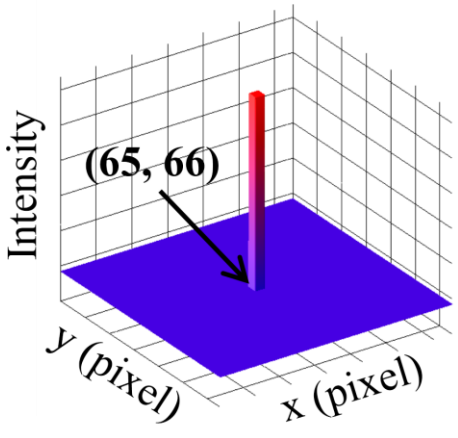

(b)

Fig. 2. (a) ROI shown on base image and deformed image (b) 3D surface plot of ROI and its surroundings

ISBN: 978-988-14047-4-9
ISSN: 2078-0958 (Print); ISSN: 2078-0966 (Online)

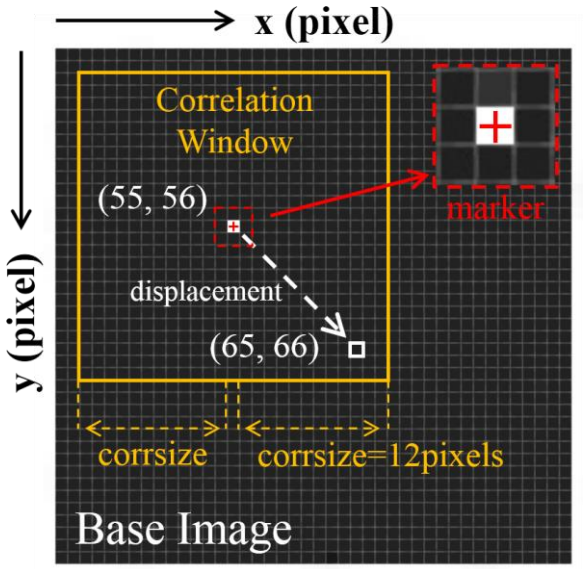

Fig. 3. Setup of DIC analysis condition when *corrsize* is 12pixels as an example

Four cases were studied where values of real displacement *d* were 1pixel, 2pixels, 5pixels and 10pixels. The position of the white pixel (as well as marker) for the four cases above are listed in Table I. It was made sure that the white pixel is on the top left part of the base image for all the four cases when preparing images for this study. Thereby, the distances between the white pixel to the right and bottom image boundaries are not influencing the results. Values of *corrsize* were chosen differently according to different *d* for DIC analysis (Fig. 4). Error factor *f* represents the normalized error level of DIC results and was calculated as follows

$$f = \sqrt{\frac{1}{2}\left[\left(\frac{dx-d}{d}\right)^2 + \left(\frac{dy-d}{d}\right)^2\right]} \quad (1)$$

where *dx* and *dy* are the displacement values along x and y respectively that DIC analysis results gave. *f*=0 means DIC results are completely correct while *f*=1 means DIC tracking is not working at all.

III. Results and Discussion

Fig. 4 demonstrates the relationship between DIC error factor and *corrsize*. It is evident that for a specific *d*, *corrsize* has a lower bound ($corrsize_{min}$) and an upper bound ($corrsize_{max}$), only between which two is DIC analysis reliable. Values of bound for different real displacement are given in Table I. It is easy to understand the existence of

TABLE I
Marker Position, Upper and Lower Bounds

	marker position	*d (pixel)*	$corrsize_{min}$	$corrsize_{max}$
Case 1	(28, 33)	1	6	12
Case 2	(28, 33)	2	4	12
Case 3	(48, 43)	5	6	20
Case 4	(53, 54)	10	11	25

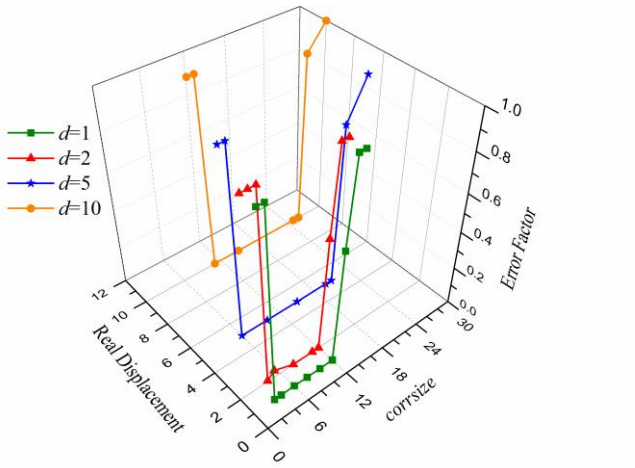

Fig. 4. The relationship between DIC result error factor, the *corrsize* and the real displacement *d*

$corrsize_{min}$: only when the correlation window is large enough to cover the real displacement, is DIC able to find the new position of ROI in the deformed image.

In principle, any value of *corrsize* larger than the real displacement should give reliable results in this case, except that larger *corrsize* takes longer analysis time. What was discovered above is related to the image boundary effect. Equation (2) summarises the criterion for the upper bound of *corrsize*

$$corrsize < l/2 - 1 \quad (2)$$

where *l* is the rounded-up number of the smallest value among the distances between the marker and the four image boundaries. Note that decimal place can exist in marker position value, and rounding-up in this case gets the nearest integer. Compare Equation (2) with Table I, good agreement can be achieved.

This DIC package was initially developed to evaluate microstrains for FIB-DIC ringcore milling experiment in combination with Scanning Image Microscopy (SEM). In that case, the real displacement is often at sub-pixel level and the ROI is normally in the middle of the image. Thereby, the lower and upper bounds studied in this paper are unlikely to affect the accuracy of DIC results. However, when it comes to situation where relatively large scale of real displacement is involved, the upper bound should serve as a criterion for the choice of *corrsize*. Additionally, efforts should be made when taking images for DIC analysis to ensure that the ROI is centred. When, in some more extreme circumstances, bringing ROI to the image centre is not an option, and in the meantime the real displacement is larger than *l*/2-1, that means DIC is unable to track the displacement using conventional analysis procedure and the original images directly. The image boundary needs to be manipulated somehow to have a wider edge without disturbing the intensity levels of the original image, e.g. putting a 'patch' with zero-intensity pixels around the original image.

IV. Conclusion

In this study the influence of correlation window size *corrsize* on the DIC results with different real displacement

ISBN: 978-988-14047-4-9
ISSN: 2078-0958 (Print); ISSN: 2078-0966 (Online)

was explored. It is found out that DIC can give sensible results when the *corrsize* is between a lower bound ($corrsize_{min}$) and an upper bound ($corrsize_{max}$). The upper bound is resulted from image boundary effect. An equation is given as a criterion for *corrsize* choice. The content in this paper is crucial when DIC analysis is utilised for cases where the distance between ROI and the image boundary is limited and the real displacement is relatively large.

ACKNOWLEDGMENT

The authors are thankful to academics who worked for project iStress for providing studying cases for the development of the DIC package used in this paper[17].

REFERENCES

[1] Pan, B., et al., *Two-dimensional digital image correlation for in-plane displacement and strain measurement: a review*. Measurement science and technology, 2009. **20**(6): p. 062001.
[2] McCormick, N. and J. Lord, *Digital image correlation.* Materials today, 2010. **13**(12): p. 52-54.
[3] Kujawińska, M., M. Malesa, and K. Malowany, *Sensing & Measurement Measuring structural displacements with digital image correlation.*
[4] Kang, J., et al., *Digital image correlation studies for microscopic strain distribution and damage in dual phase steels.* Scripta Materialia, 2007. **56**(11): p. 999-1002.
[5] Vendroux, G. and W. Knauss, *Submicron deformation field measurements: Part 2. Improved digital image correlation.* Experimental Mechanics, 1998. **38**(2): p. 86-92.
[6] Korsunsky, A.M., M. Sebastiani, and E. Bemporad, *Residual stress evaluation at the micrometer scale: analysis of thin coatings by FIB milling and digital image correlation.* Surface and Coatings Technology, 2010. **205**(7): p. 2393-2403.
[7] Sebastiani, M., et al., *Depth-resolved residual stress analysis of thin coatings by a new FIB–DIC method.* Materials Science and Engineering: A, 2011. **528**(27): p. 7901-7908.
[8] Lunt, A.J., et al., *A state-of-the-art review of micron-scale spatially resolved residual stress analysis by FIB-DIC ring-core milling and other techniques.* The Journal of Strain Analysis for Engineering Design, 2015: p. 0309324715596700.
[9] Sun, Z., J.S. Lyons, and S.R. McNeill, *Measuring microscopic deformations with digital image correlation.* Optics and Lasers in Engineering, 1997. **27**(4): p. 409-428.
[10] Zhang, H., et al. *Effect of Pt Deposition on Digital Image Correlation Analysis for Residual Stress Measurement Using FIB-DIC Ringcore Method*. in *Proceedings of the World Congress on Engineering*. 2016.
[11] Prime, M.B., *Residual stress measurement by successive extension of a slot: the crack compliance method.* Applied Mechanics Reviews, 1999. **52**: p. 75-96.
[12] Mansilla, C., et al., *On the determination of local residual stress gradients by the slit milling method.* Journal of Materials Science, 2015. **50**(10): p. 3646-3655.
[13] Sabate, N., et al., *Residual stress measurement on a MEMS structure with high-spatial resolution.* Journal of microelectromechanical systems, 2007. **16**(2): p. 365-372.
[14] Winiarski, B. and P. Withers, *Micron-scale residual stress measurement by micro-hole drilling and digital image correlation.* Experimental mechanics, 2012. **52**(4): p. 417-428.
[15] Krottenthaler, M., et al., *A simple method for residual stress measurements in thin films by means of focused ion beam milling and digital image correlation.* Surface and Coatings Technology, 2013. **215**: p. 247-252.
[16] Keil, S., *Experimental Determination of Residual Stresses with the Ring-core Method and an On-line Measuring System.* Experimental Techniques, 1992. **16**(5): p. 17-24.
[17] Senn, M. and C. Eberl. *Digital Image Correlation and Tracking*. 2015; Available from: https://uk.mathworks.com/matlabcentral/fileexchange/50994-digital-image-correlation-and-tracking.
[18] Lunt, A.J. and A.M. Korsunsky, *A review of micro-scale focused ion beam milling and digital image correlation analysis for residual stress evaluation and error estimation.* Surface and Coatings Technology, 2015. **283**: p. 373-388.
[19] Matlab. *normxcorr2*. Available from: https://uk.mathworks.com/help/images/ref/normxcorr2.html.
[20] Lewis, J. *Fast normalized cross-correlation*. in *Vision interface*. 1995.

ISBN: 978-988-14047-4-9
ISSN: 2078-0958 (Print); ISSN: 2078-0966 (Online)